Molecular Crystals and Liquid Crystals
Publication details, including instructions for authors and subscription information:
http://www.tandfonline.com/loi/gmcl16

Flexoelectricity in the Hybrid Aligned Nematic Cell

B. Valenti [a d], C. Bertoni [a], G. Barbero [b d], P. Taverna-Valabrega [b] & R. Bartolino [c d]

[a] Istituto di Chimica Industriale, Università di Genova, 16132, Genova, Italy

[b] Dipartimento di Fisica, Politecnico di Torino, 10129, Torino, Italy

[c] Unical Liquid Crystal Group, Dip. di Fisica, Università della Calabria, 87036 Arcavacata di Rende, Cosenza, Italy

[d] GNSM-CISM Unità di Cosenza Arcavacata di Rende, Cosenza, Italy

Version of record first published: 13 Dec 2006.

To cite this article: B. Valenti , C. Bertoni , G. Barbero , P. Taverna-Valabrega & R. Bartolino (1987): Flexoelectricity in the Hybrid Aligned Nematic Cell, Molecular Crystals and Liquid Crystals, 146:1, 307-320

To link to this article: http://dx.doi.org/10.1080/00268948708071820

Mol. Cryst. Liq. Cryst., 1987, Vol. 146, pp. 307–320
Photocopying permitted by license only

Printed in the United States of America

Flexoelectricity in the Hybrid Aligned Nematic Cell

B. VALENTI,† C. BERTONI

Istituto di Chimica Industriale, Università di Genova, 16132 Genova—Italy

and

G. BARBERO,† P. TAVERNA-VALABREGA

Dipartimento di Fisica, Politecnico di Torino, 10129 Torino—Italy

and

R. BARTOLINO†

Unical Liquid Crystal Group, Dip. di Fisica, Università della Calabria, 87036 Arcavacata di Rende, Cosenza—Italy

(*Received August 6, 1986; in final form December 8, 1986*)

The reorientation process of an HAN cell submitted to electric fields is studied both theoretically and experimentally. To isolate the flexoelectric effect from the dielectric one, the experiments are made under d.c. and a.c. excitations. Preliminary results on 6 μm thick MBBA have been reported. In this paper we investigate the influence of the thickness in the range between 3 and 15 μm for MBBA. The theoretical model includes into the free energy the flexoelectric term in the hypothesis that the true inner electric field is due to the effective conduction anisotropy. In such a way we derive simultaneously from the experiments the surface anchoring energy and the sum of the flexoelectric coefficients; the found values are in good agreement with those derived by other groups with different techniques.

Keywords: flexoelectricity, hybrid cell, reorientation, anchoring energy, electrooptics, flexoelectric coefficients

INTRODUCTION

A hybrid aligned nematic (HAN) sample is obtained when the two glass surfaces of a cell are treated to induce, respectively, homeotropic

†GNSM-CISM Unità di Cosenza Arcavacata di Rende, Cosenza—Italy.

and planar alignments.[1-3] We analyze the molecular reorientation of this cell submitted to an electric field applied parallel to the deformation plane and perpendicular to the glass boundaries; in this geometry, under a.c. fields, there is no threshold for the appearance of the electro-optical effects.[1]

In a first paper[4] we noticed that the main contribution to the molecular reorientation of a HAN cell excited by a.c. voltages arises from the dielectric term in the free energy; to explain qualitatively the anomalous behavior evidenced in the d.c. case at low fields we took into account the flexoelectric characteristics of the examined cell.

A successive investigation[5] evidenced this last effect; the theoretical curve derived by including the flexoelectric term in the total free energy appeared to be in good agreement with the experimental behavior of a 6 μm cell of MBBA doped with a small amount of an electrochemical standard material. To justify the experimental results obtained with undoped MBBA we assumed a low voltage screening of the applied electric field due to the presence of ionic impurities in the material; this interpretation was in line with the idea of Madhusudana and Durand,[6] who attributed to the screening by counterions the non linearity observed at low voltage in the electrically-controlled birefringence of a similar cell.

In the present paper we report a systematic investigation of the influence of the cell thickness on the a.c. and d.c. electro-optical behavior of HAN cells of MBBA. To better clarify the role played at low voltages by both the flexoelectric and the screening effects we improve the experimental accuracy of our measurements and critically consider the effect of slight variations in some of the parameters involved, first of all the cell thickness. The theoretical model includes into the free energy the flexoelectric term, in the hyphotesis that the true inner electric field is due to the effective conduction anisotropy.[5]

EXPERIMENTAL

MBBA slabs of various thicknesses (ranged between 3 and 15 μm) have been sandwiched between two conductive glass surfaces coated respectively with ODS-E by Chisso Co. (homeotropic alignment) and a polymeric thin film of formvar (planar alignment), as previously described.[4,5,7] The experimental arrangement used is schematized in Figure 1. The cells have been analyzed between two crossed polarizers, as in Refs. 4 and 5, using a He-Ne laser as light source and a

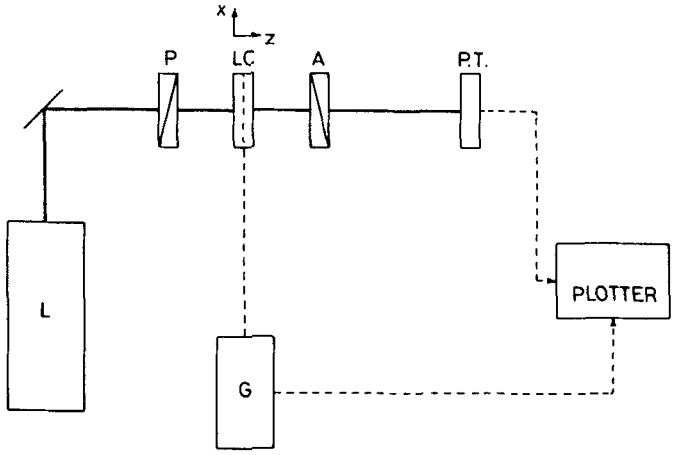

FIGURE 1 Schematic representation of the experimental arrangement (*L*: He-Ne laser, *P*: polarizer, *A*: analyzer, *LC*: sample, *P.T.*: phototransistor, *G*: saw tooth or a.c. generator)

phototransistor of high sensitivity to detect the transmitted light intensity; the whole recordering system is fully automated.

All the cells have been investigated using a 500 Hz a.c. sinewave (0–5 volts) and a d.c. power source (0–8 volts). The rate of increasing of the applied voltage has been maintained constant and not exceeding the value of 5×10^{-3} V/sec. As discussed in a previous paper,[5] on the basis of the characteristic times, we can consider that all the measurements are taken under thermodinamic equilibrium conditions.

The role played by the flexoelectric effect has been investigated by comparing a.c. measurements with the d.c. behavior under positive and negative voltages. To verify the hypothesis of a screening effect by counterions we have examined at any thickness the behavior of undoped MBBA and of MBBA doped with a small amount (2×10^{-3} Ml^{-1}) of ferrocene (bicyclopentadienyliron).

Figures 2–6 show the experimental trends of the transmitted light intensity against the applied a.c. and d.c. voltage for mylar thicknesses of 3, 9 and 15 μm in cells of undoped MBBA (Figures 2, 5 and 6) and for 4 and 6 μm spaced cells of MBBA additioned with ferrocene (Figures 3 and 4). The transmitted light intensity is normalized as $I^* = (I-I_{min})/(I_{max}-I_{min})$, where I_{max} and I_{min} are respectively the higher and the lower intensity value of the whole set of data (common for the a.c. and d.c. curves belonging to the same thickness). The shape of the d.c. curves appears to be strongly affected by the polarity

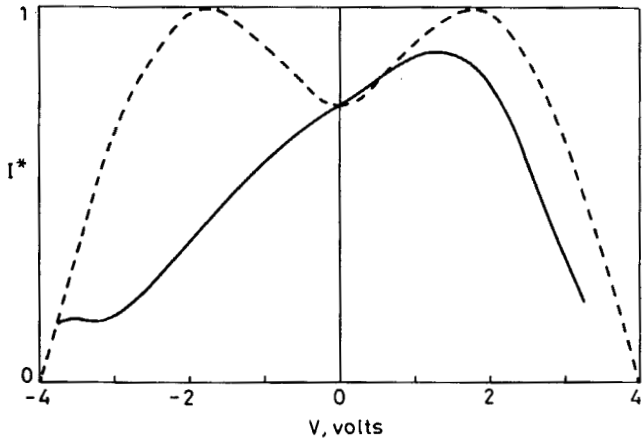

FIGURE 2 Intensity of the transmitted light under d.c. (solid curve) and a.c. (dotted line) voltages for an undoped MBBA cell of 3 μm.

of the applied field and by the thickness of the cell, but no appreciable difference seems to be evidenced by the comparison between doped and undoped cells. Responses under d.c. positive voltages (i.e. when the planar wall is connected to the plus of the generator) are very close to the a.c. ones, as shown on the right hand sides of Figures

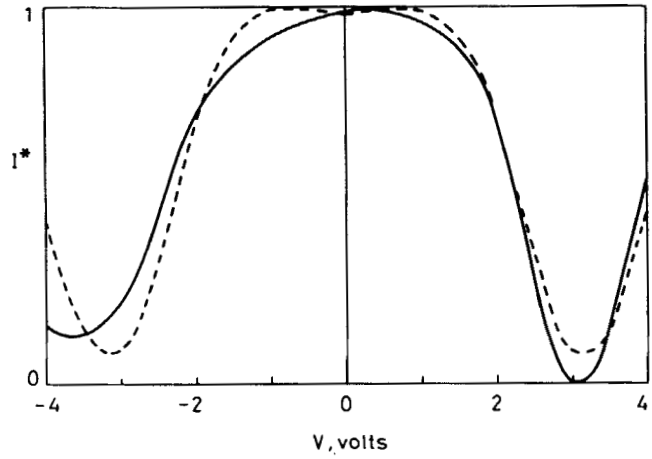

FIGURE 3 MBBA doped with ferrocene, $d = 4$ μm.

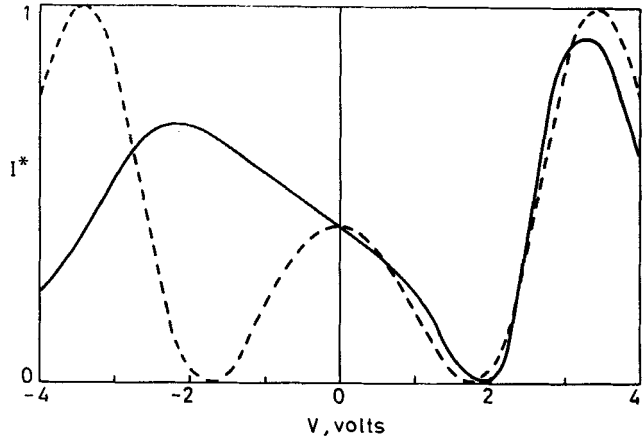

FIGURE 4 MBBA doped with ferrocene, $d = 6$ μm.

2–6; when the applied voltage is negative d.c. and a.c. curves differ mainly for thinner samples. The linear response region around zero voltage is strongly asymmetric and becomes shorter when the cell thickness is increased. From our measurements it is also evident that, by changing the rate of increasing of the applied voltage, the re-orientation process of the system is more rapid for thinner samples.

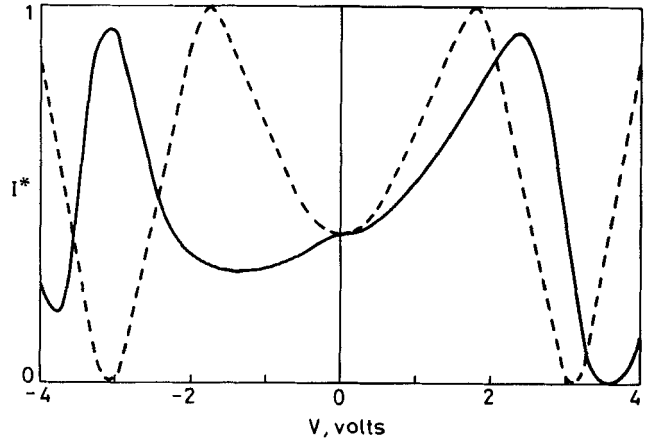

FIGURE 5 Undoped MBBA, $d = 9$ μm.

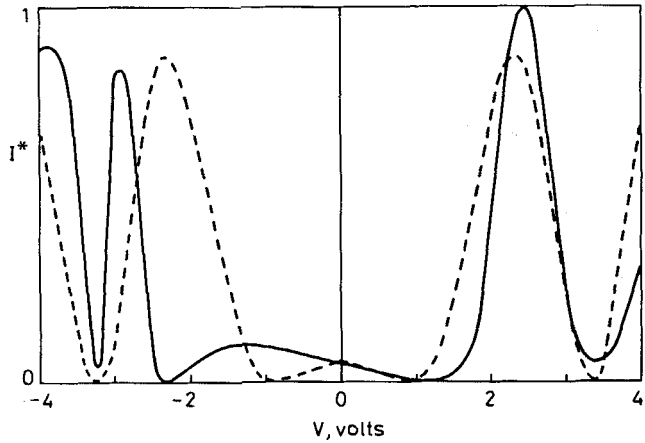

FIGURE 6 Undoped MBBA, $d = 15$ μm.

THEORY AND DISCUSSION

A detailed theoretical analysis have been reported in Ref. 5. In this paper we review briefly the hypotheses on which the treatment is based and the fundamental equations.

1. The liquid crystal is assumed to be a conductor, with Debye screening length L_D[8] much smaller than the sample thickness d; therefore the diffusion current is negligible in the medium.
2. The electrodes are supposed to be ideal; hence the charge transfer from surface ions is instantaneous and uniform.
3. The dissipation function of the steady problem is assumed to be given only by $R = \sigma_{ij}(\phi)\, E_i E_j$, where ϕ is the tilt angle between the director **n** and the z axis, σ_{ij} the conductivity tensor and E_i, E_j the electric field components. Then the viscous torque is $\partial R/\partial(\partial\phi/\partial t) \equiv 0$ and the problem is a static one. The only role of the dissipation is to fix the potential distribution through the $\sigma_{ij}(\phi)$ dependence.
4. The tilt angles are supposed to be small; as a consequence terms in ϕ^4 are neglected.
5. For sake of simplicity the splay and bend elastic constants are assumed to be equal $k_{11} = k_{33} = k$ (one-constant approximation).[9]
6. The anchoring energy W on the homeotropic wall is infinitely large (silane treatment[10]), but it is small on the planar boundary (formvar treatment).

The intensity of the transmitted light for normal incidence can be written in the form

$$I = I_o \sin^2\left(\frac{\pi}{\lambda}\Delta l\right) \tag{1}$$

where Δl is the optical path difference between the ordinary and the extraordinary ray. In the frame of the previous hypotheses Δl can be evaluated as the sum of the contributions from thin layers of the crystals of thickness dz

$$\Delta l = n_o\left[\int_o^d (l - R\sin^2\phi)^{-1/2}dz - d\right] \tag{2}$$

with $R = 1 - (n_o/n_e)^2$.

On the other hand, from hypotheses 1 and 3, the voltage can be written as

$$V = \frac{\xi}{\sigma_\parallel}\mu\int_o^{\Phi_2}[(1-\sigma\sin^2\phi)\,(1-\mu^2-\sigma\sin^2\phi)]^{-1/2}d\phi \tag{3}$$

In Eq. (3) $\xi = 2\pi\sqrt{\pi k\sigma/-\epsilon_a}$, where k is the elastic constant, $\epsilon_a = \epsilon_\parallel - \epsilon_\perp$ the dielectric anisotropy, $\sigma = 1-(\sigma_\perp/\sigma_\parallel)$ the relative conductivity anisotropy and $\mu = j_3/B\xi$. j_3 is the electric current density in the z direction and B can be determined by resolving the equation which gives the orientational deformations of the director profile with the boundary conditions characteristic of the HAN cell.[5]

As we have shown in Ref. 5, in the previous hypotheses, the effective anchoring energy W^* is found to be

$$W^* = W - J_3\,\bar{e}/\sigma \tag{4}$$

where W is the anchoring energy on the planar plate due only to the nematic-substrate interaction. The above mentioned relation (4) intrinsically introduces an asimmetry in the light intensity response when positive and negative voltages are applied. In fact, if $\bar{e} > 0$ for $J_3 > 0$ (i.e. $V > 0$), W^* is greater than W. Therefore the planar configuration on the wall is stabilized. Since $\epsilon_a < 0$, the effect of the electric field on the medium favours the planar orientation. It follows that, in a.c. and d.c. current with $V > 0$, the trends are similar. On the other hand, if $J_3 < 0$, W^* results smaller than W and hence the

anchoring energy decreases when the intensity of the electric field increases. In this region the electric effects on the surface and in the bulk are opposite. This fact implies that, in the case of MBBA, only for $V < 0$ the trends in a.c. and d.c. current must be considerably different.

In Figure 7 we show the light intensity I* against the voltage for three different values of the thickness d (3.2, 6.3 and 9.5 μm); these curves are obtained by numerical calculations. The values of the MBBA parameters involved are indicated in the figure caption. Figure 8a refers to the I* vs. V plot in a 7.4 μm sample for two values of the ratio w/k; a 10% variation of w/k gives rise to a 25% shift in the left hand side of the I curve and in the I* value at V = 0 and therefore appears to be easily detectable. Moreover, in Figure 8b, which refers again to a 7.4 μm cell, we plot I* vs. V for two values of $\tilde{e}/k$ ($\tilde{e} = e_{11} + e_{33}$ is the sum of the flexoelectric coefficients); a 10% variation of $\tilde{e}/k$ results in a 8% additional displacement of the maximum position, which cannot be attributed to an inexact evaluation of w/k, because I* (V = 0) does not depend upon $\tilde{e}/k$. We emphasize that, using this new method of analyzing the I curves vs. voltage, we can derive the values of the ratios $\tilde{e}/k$ and w/k. It must be noticed that only the left hand sides of the plots (I vs. negative voltages) are useful for the evaluation of the ratios e/k and w/k since,

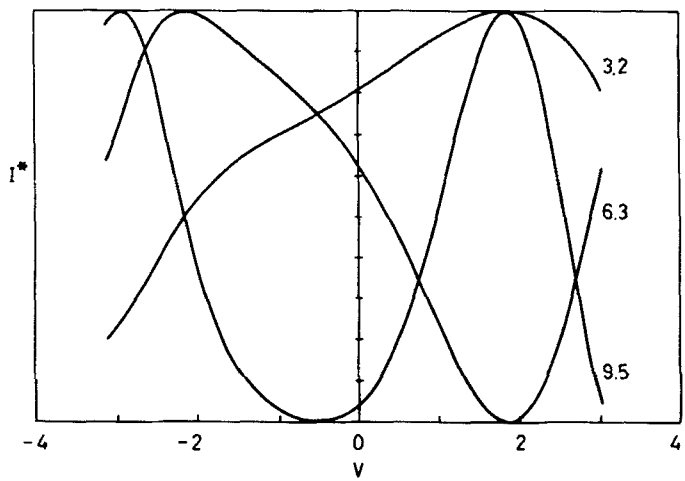

FIGURE 7 Calculated curves for 3.2, 6.3 and 9.5 μm cells of MBBA ($\epsilon_a = -0.7$[11]. $\sigma_\parallel = 6\times10^{-11}$ $(\Omega\ \text{cm})^{-1}$,[12] $\sigma_\perp = 4\times10^{-11}$ $(\Omega\ \text{cm})^{-1}$,[12] $\sigma = 0.32$, $\lambda = 0.6328$ μm, $k = 7\times10^{-7}$ dynes,[13] R = 0.207,[13] $n_o = 1.57$[13]).

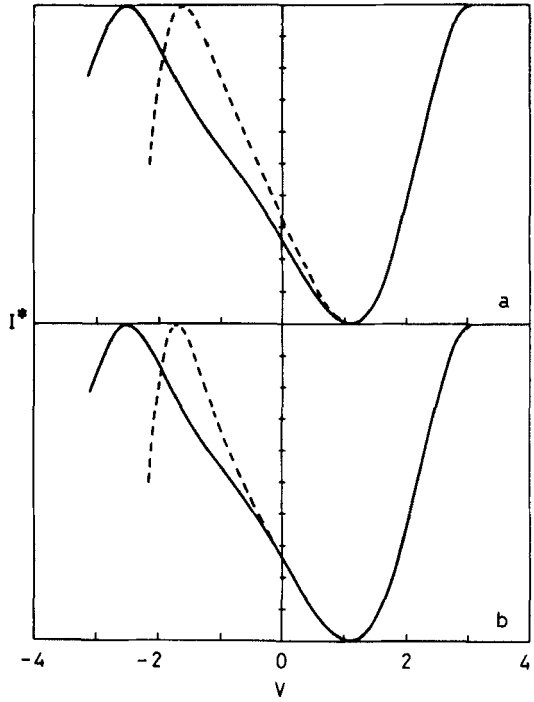

FIGURE 8 Calculated curves for a 7.4 μm cell of MBBA. Shifts (dotted lines) are due to 10% variations of w/k (Figure 8a) and $\tilde{e}/k$ (Figure 8b).

as already mentioned,[5] the effective anchoring energy is lowered and the small tilt angle approximation is mainly valid only in this region.

A method described by some of the authors in Ref. 14 permits to measure the Frank elastic constants by light scattering differential-cross-section measurements, with an error which ranges from 2% up to 5%. Of course, if the elastic constant k is preventively determined with this last procedure,[14] the method presented here allows us to evaluate $\tilde{e}$ and w with an indetermination of about 20% which is, in this kind of measurements, an upper limit.

Finally, in Figures 9–13 we report a series of fits I* vs. V which describe the pattern of interference fringes for the five samples of figures 2–6. The full lines, derived by using Eqs. 1 and 2 for the intensity and by numerically integrating Eq. 3 to obtain the voltage, are the best fits of the experimental points (also indicated in the figures). Let us underline that the free parameters of the fits are in principle the following: $\tilde{e}/k$, w/k and the thickness d, with the physical constrain coming from the fact that the parameters $\tilde{e}/k$ and w/k must

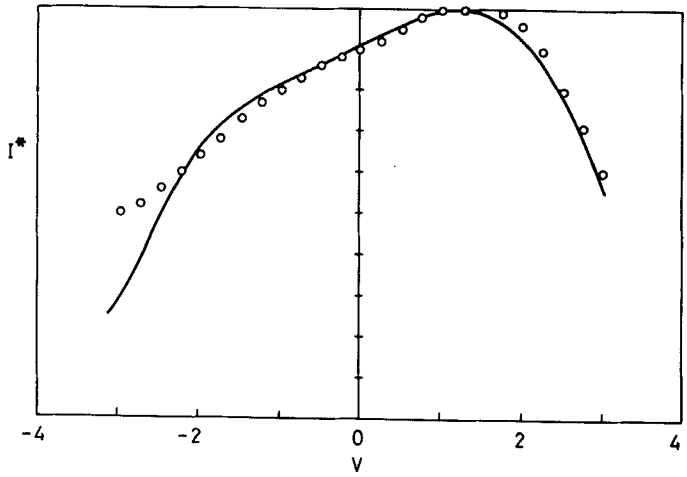

FIGURE 9 Fit of the d.c. results of Figure 2 normalized as I* between the maximum and the minimum intensity values of the first oscillation in d.c., around zero voltage. Extimated thickness 3.6 μm.

be the same at any sample thickness. On the other hand the real sample thickness cannot be known with an accuracy better than 10–15%, because of the initial uncertainty on the mylar sheet thickness, its mechanical properties (see also Ref. 15) and finally the sample preparation (capillarity effect and so on).

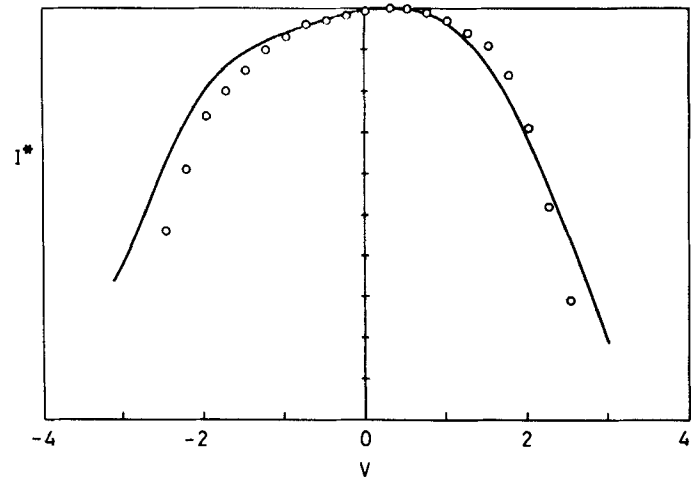

FIGURE 10 Fit of the d.c. results of Figure 3. Extimated thickness 4.2 μm.

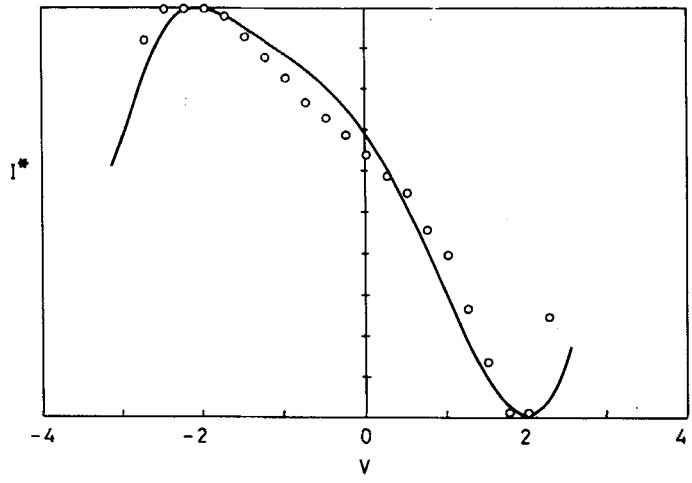

FIGURE 11 Fit of the d.c. results of Figure 4. Extimated thickness 6.1 μm.

Therefore we choose $\tilde{e}/k$ and w/k in such a way that they can fit simultaneously all the experimental curves and vary slightly d in order to find the "real" sample thicknesses. The evaluated values of the ratios w/k and $\tilde{e}/k$ are:

$$w/k = (0.83 \pm 0.17) \times 10^4 \text{ cm}^{-1}$$

$$\tilde{e}/k = -(0.75 \pm 0.15) \times 10^3 \text{ dynes}^{0.5} \text{ cm}^{-2}$$

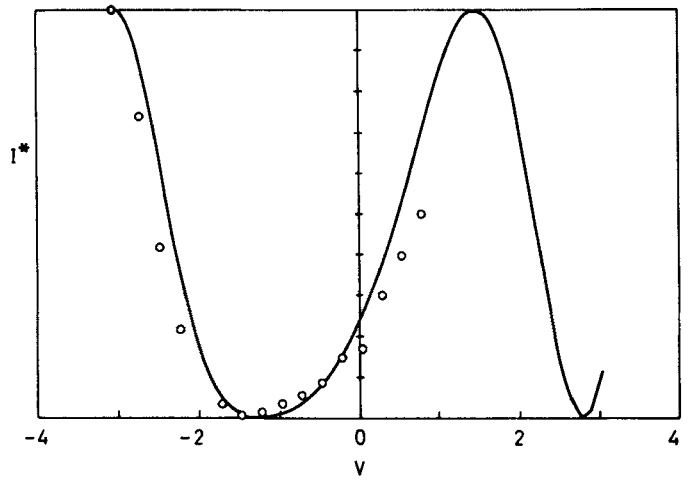

FIGURE 12 Fit of the d.c. results of Figure 5. Extimated thickness 10.3 μm.

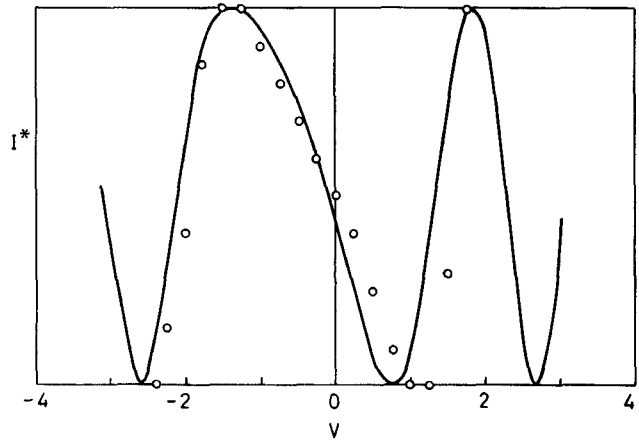

FIGURE 13 Fit of the d.c. results of Figure 6. Extimated thickness 15.8 μm.

The extimated "real" thicknesses of the cells are indicated in the figure captions.

The last point we have to discuss relates to the apparent disagreement between some results of Ref. 5 and some of those reported in this paper, as far as the comparison between doped and undoped MBBA samples is concerned. In effect we do not observe a systematic difference in the behavior of several doped and undoped HAN cells of the same thickness. This fact probably happens because commercial MBBA always contains impurities arising from degradation which mask ferrocene effects. After a critical reexamination of all our data, we think that the following points must be taken into account: i) the improved accuracy of the measurements (higher sensitivity of the detector and observation of a reduced area due to the use of a laser beam) allows us to reveal very small variations of the transmitted intensity; ii) the use of a more adequate normalization criterion results in a better understanding of the experimental behaviors. In Ref. 5 normalized I* values have been derived by assuming for I_{max} and I_{min} the highest and the lowest I data determined in the measurement range. However in Figures 9–13 we show that the better comparison between calculated and experimental curves is attained by normalizing the latter between the maximum and the minimum of the first oscillation, around zero voltage; iii) in the previous papers we considered the spacer thickness as the true thickness of the cells. Now we have shown that, in the actual accuracy, the thickness must be kept as a slightly adjustable parameter. On the basis of these com-

ments, when the exact normalization is adopted, it seems reasonable to evaluate first if small differences between experimental curves can be attributed to an inexact extimation of the cell thickness, before to take into account other effects. To check the role played by small amounts of ferrocene on the electrochemical behavior of MBBA we have probably to examine samples of the liquid crystal containing smaller amounts of impurities. In our case measurements of relative conductivity appear to be practically the same for doped and undoped MBBA.

CONCLUSIONS

We have measured the intensity of the transmitted light through hybrid cells of MBBA of different thickness when an electric field is applied.

A rather new numerical analysis of the experimental results allows us to evaluate simultaneously the ratios w/k and $\tilde{e}/k$.

By evaluating the elastic constant from literature data, we calculate the absolute values of the anchoring energy ($w = (5.8 \pm 0.9) \times 10^{-3}$ erg/cm^2) and of the flexoelectric coefficient ($\tilde{e} = -(4.5 \pm 0.7) \times 10^{-4}$ dynes$^{0.5}$). These results, whose order of magnitude is in agreement with that determined by other groups with different techniques[16-18] ($\tilde{e} = -7 \times 10^{-4}$ dynes), are derived with a good accuracy.

Our method can be extended to various liquid crystals. This last aspect is important since $\tilde{e}$ is generally unknown. $\tilde{e}$ can give informations on the surface polarization of different materials. Checks of the model for several liquid crystals with different dielectric anisotropies are in progress, as well as the dynamical aspects of the reorientation.

Acknowledgment

We acknowledge Dr. C. Versace for his help in the experimental set-up mounting.

References

1. S. Matsumoto, M. Kawamoto and K. Mizunoya, *J. Appl. Phys.*, **47**, 3842 (1976).
2. G. Barbero, F. Simoni and P. Aiello, *J. Appl. Phys.*, **55**, 304 (1984).
3. I. Dozov, Ph. Martinot-Lagarde and G. Durand, *J. Physique Lett.*, **43**, 365 (1982); and *J. Physique Lett.*, **44**, 817 (1983).

4. E. Antolini Calcagno, B. Valenti, G. Barbero, R. Bartolino and F. Simoni, *Mol. Cryst. Liq. Cryst.*, **127**, 215 (1985).
5. G. Barbero, P. Taverna-Valabrega, R. Bartolino and B. Valenti, *Liq. Cryst.*, **1**, 483 (1986).
6. N. V. Madhusudana and G. Durand, *J. Physique Lett.*, **46**, 195 (1985).
7. F. Simoni, R. Bartolino, G. Barbero, P. Aiello and B. Valenti, *Mol. Cryst. Liq. Cryst.*, **113**, 303 (1984).
8. L. M. Blinov, "*Electro-optical and Magneto-optical Properties of Liquid Crystals*" (J. Wiley and Sons, New York, 1983), Chap. 5, pp. 159–161.
9. P. G. de Gennes, "*The Physics of Liquid Crystals*" (Oxford University Press, Oxford, 1974), Chap. 3, pp. 82–85.
10. G. Barbero, N. V. Madhusudana and G. Durand, *J. Physique Lett.*, **45**, 613 (1984).
11. D. Diguet, F. Rondelez and G. Durand, *C. R. hebd. Séanc., Acad. Sci.*, Paris, **B-271**, 954 (1970).
12. H. Kelker and R. Hatz, *Handbook of Liquid Crystals* (Verlag Chemie, Weinheim, (1980).
13. C. Oldano, E. Miraldi, A. Strigazzi and P. Taverna-Valabrega, *J. Physique Lett.*, **45**, 355 (1984).
14. E. Miraldi, C. Oldano, P. Taverna-Valabrega and L. Trossi, *Il Nuovo Cimento*, **66B**, 179 (1981).
15. H. Takezoe, Y. Ouchi, M. Hara, A. Fukuda and E. Kuze, *Jpn. J. Appl. Phys.*, **22**, 1080 (1983).
16. J. P. Marcerou and J. Prost, *Mol. Cryst. Liq. Cryst.*, **58**, 259 (1980).
17. I. Dozov, I. Penchev, Ph. Martinot-Lagarde and G. Durand, *Ferroelectr. Lett.*, **2**, 135 (1984).
18. H. P. Hinov and A. I. Derzhanski, "*Liquid Crystals & Ordered Fluids*," A. C. Griffin and J. F. Johnson, eds. (Plenum Press, New York, 1984), vol. 4, p. 1103.